35th Annual International Conference of the IEEE EMBS
Osaka, Japan, 3 - 7 July, 2013

3-D Segmentation of Human Sternum in Lung MDCT Images

Banafsheh Pazokifard
School of Computer Science and Engineering
University of New South Wales
Sydney, New South Wales, 2052, Australia
Email: bpazoki@cse.unsw.edu.au

Arcot Sowmya
School of Computer Science and Engineering
University of New South Wales
Sydney, New South Wales, 2052, Australia
Email: sowmya@cse.unsw.edu.au

***Abstract*— A fully automatic novel algorithm is presented for accurate 3-D segmentation of the human sternum in lung multi detector computed tomography (MDCT) images. The segmentation result is refined by employing active contours to remove calcified costal cartilage that is attached to the sternum. For each dataset, costal notches (sternocostal joints) are localized in 3-D by using a sternum mask and positions of the costal notches on it as reference.**

The proposed algorithm for sternum segmentation was tested on 16 complete lung MDCT datasets and comparison of the segmentation results to the reference delineation provided by a radiologist, shows high sensitivity (92.49%) and specificity (99.51%) and small mean distance (dmean=1.07 mm). Total average of the Euclidean distance error for costal notches positioning in 3-D is 4.2 mm.

I. INTRODUCTION

Accurate segmentation and 3-D modeling of the sternum in multi detector computed tomography (MDCT) images is a clinically valuable goal. The precisely segmented sternum is a stable reference for registration of chest images, analysis of human anatomy and localization of the costal notches (sternocostal joints) in 3-D. In addition, it contributes to sternum implant surgery and pre- and post-surgical analysis related to sternum deformity correction surgery. Costal notches positioning helps to estimate the costal cartilage centre points from costochondral joint (CCJ) to the sternum more accurately.

A model of the sternum has been presented [1] based on geometry and used to fabricate an implant. The algorithm uses healthy sternum samples to generate clouds of points and a polygonal model. The technique to extract the sternum samples includes thresholding, region growing and editing. However the details and accuracy of the sternum samples' segmentation have not been provided.

To extract pleural effusion in CT images, the sternum has been used for registration [2]. 3-D sternum was obtained by setting a regular triangle ROI at the anterior region and extending it to VOI in z direction, yet performance of the sternum segmentation has not been discussed.

Another method [3] uses the sternum and costal notches information in 3-D to approximate the costal cartilage both before and after sternum displacement, without providing the sternum segmentation technique and accuracy evaluation.

To sum up, limited attempts have been made on sternum segmentation to date. In related publications, sternum segmentation is a part of other segmentation and to our knowledge, no other published work has focused specifically on sternum segmentation and evaluation.

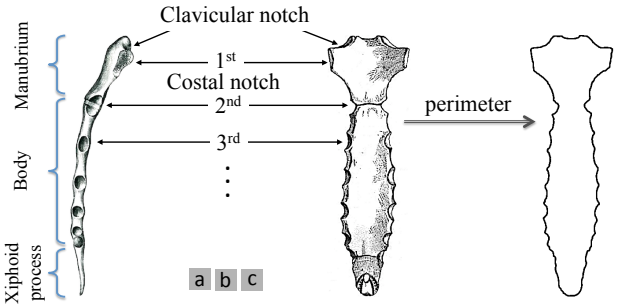

Fig. 1. (a) and (b) sternum side and front-view [4], (c) 2-D sternum mask

The main contributions of this paper are: (i) a novel algorithm for sternum segmentation in modern lung MDCT images and (ii) localization of costal notches in 3-D. Our fully automatic algorithm is a novel way to segment and isolate the sternum in 3-D in lung MDCT datasets, followed by a novel method to refine the segmentation result. For refinement, we use the perimeter of the sternum front-view (Figure 1 (b)) as illustrated in Gray's anatomy [4]. By using the sternum perimeter as sternum mask, existing calcified cartilage that is attached to the sternum is removed automatically. Finally using pre-knowledge of costal notches locations on the 2-D sternum mask, we localize 14 costal notches in each dataset in 3-D in Cartesian coordinate system.

The remaining paper is summarized as follows: in section II, an overview of the proposed algorithm including bone segmentation and sternum isolation in 3-D is presented. This section also includes the novel framework to refine the segmentation result, and the method of costal notch localization in 3-D is explained in II-D. The experimental results and evaluations are discussed in section III and the paper ends with conclusion and discussion in section IV.

II. PROPOSED SEGMENTATION FRAMEWORK

The first step in sternum segmentation is to extract the bone structure in the lung MDCT dataset. We employ the well-known graph cuts algorithm for chest bone segmentation in 3-D [5]. After extracting the whole bone in MDCT dataset, the next step is to automatically segment and isolate

978-1-4577-0216-7/13/$26.00 ©2013 IEEE

the sternum in 3-D. The result of sternum segmentation may include existing calcified costal cartilage. To exclude the irrelevant structures and identify the sternum border, the active contours model is employed. By taking advantage of knowledge about sternum anatomy, we localize the costal notches in 3-D. The whole framework and detailed steps are summarized in Figure 2 with an example for each step.

A. Chest Bone Segmentation

The first step is to prepare MDCT images of the dataset for bone segmentation. This includes: (i) converting the MDCT images to a conventional image format, (ii) removing extraneous pixels such as air and other artifacts around the body with thresholding and (iii) segmenting the lungs, using graph cuts [6], and removing them in MDCT datasets, as they do not carry helpful data for bone segmentation.

After preparing the datasets for bone segmentation, graph cuts algorithm [7] is employed as a fast and effective way to extract high contrast bone structure from the dataset [5].

For our purpose, bones in lung MDCT dataset and other soft tissues are chosen as object and background respectively to build the weighted graph $G = \langle V, E \rangle$. In mathematical terms, optimal image segmentation is optimal pixels/voxels labeling via minimizing the following energy function [8]:

$$E(A) = \lambda . \sum_{p \in P} R_p(A_p) + \sum_{\{p,q\} \in N} B_{p,q} \cdot \delta_{A_p \neq A_q} \quad (1)$$

The regional part R_p, for both bone and soft tissue is defined as a Gaussian function. Expectation maximization (EM) algorithm is employed to estimate the parameter values of the Gaussian functions. The pixels/voxels intensity value and the estimated Gaussian function values are passed to graph cuts algorithm to segment the chest bone in MDCT (Figure 2.a). Here, the graph G is built in 3-D with 26 neighbors. More details of graph cuts algorithm and bone segmentation in lung MDCT images may be found [5], [9].

B. 3-D Sternum Isolation

3-D result of bone segmentation in lung MDCT images includes the vertebral column, ribs, sternum, clavicle and scapula. It may also include existing calcified xiphoid process and calcified costal cartilage (Figures 2.a).

The sternum may be isolated from other bones in 3-D with 4 steps: i) ignoring the half-back of the 3-D bone segmentation result (Figure 2.b), ii) finding N number of bone cross-sections in mid-coronal plane (Figure 2.c), iii) tracing all the N objects forward and removing them at each step and iv) applying size constraint to stop the tracing procedure for each N objects. The result of this 4-step procedure is the isolated sternum in 3-D (Figure 2.d) which may include calcified costal cartilage, that should be removed.

C. Segmentation Refinement

The result of sternum isolation may include calcified costal cartilage. By employing an active contours model, we propose a novel algorithm to remove the undesired parts from the sternum segmentation result.

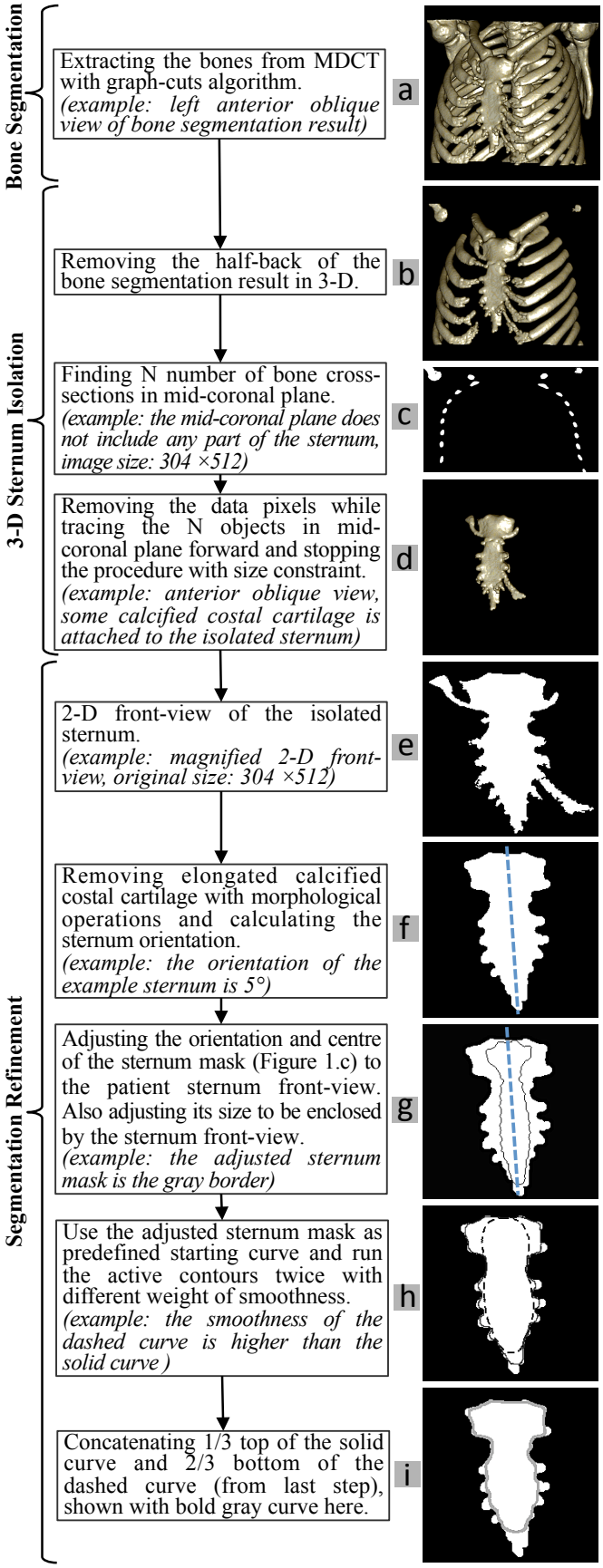

Fig. 2. Steps of sternum segmentation, tested on patient no. 7

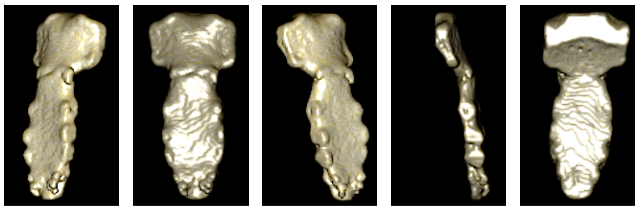

Fig. 3. Sternum segmentation in patient no. 7 MDCT dataset in different views. Left to right: left anterior oblique, anterior, right anterior oblique, right lateral and posterior views.

Active contours, originally called snakes [10], is an energy-minimizing spline that delineates objects in a given image I_0. Starting from a predefined contour, the spline curve is guided towards image features such as edges. More details of the classic active contours may be found [10], [11], [12].

The proposed algorithm to remove the calcified costal cartilage from sternum segmentation results in 3-D is summarized as follows:

(i) Add binarized coronal planes together to get 2-D front-view of the isolated sternum (Figure 2.e).

(ii) Calculate θ, the orientation of the sternum front-view. Since the elongated calcified costal cartilages attached to the sternum may change the sternum orientation significantly, they are removed by applying morphological operations (Figure 2.f).

(iii) Adjust the orientation of the sternum mask (Figure 1.c) to θ. Also, move its centre to the centre of the sternum front-view.

(iv) Adjust the sternum mask size to be enclosed by the border of the sternum front-view (Figure 2.g).

(v) Set the sternum mask as predefined starting curve for 2-D active contours. Run the active contours algorithm twice. First, run it with low weight of smoothness to define the manubrium (the sternum upper part) border. The weight of the smoothing term is chosen so that the starting curve moves toward the manubrium details well enough. In that case, the moving curve enters the calcified costal cartilages at the costal notches positions (Figure 2.h, solid curve). Second, run the active contours with higher weight of smoothing term to define the border of the sternum body more accurately (Figure 2.h, dashed curve). The final result of segmentation refinement is the concatenation of one-third top of the first active contour result and bottom two-third of the second active contour result (Figure 2.i).

(vi) Apply the result of last step to all coronal planes of the isolated sternum and remove pixel data outside it in sagittal and axial directions. Different views of the final sternum segmentation, tested on patient number 7, are in Figure 3. More examples showing removal of calcified costal cartilage from the 3-D segmentation results are in Figure 4.

D. Costal Notches Localization in 3-D

To determine the position of the 14 costal notches in 3-D, we use the sternum mask from Figure 1.c and manually mark

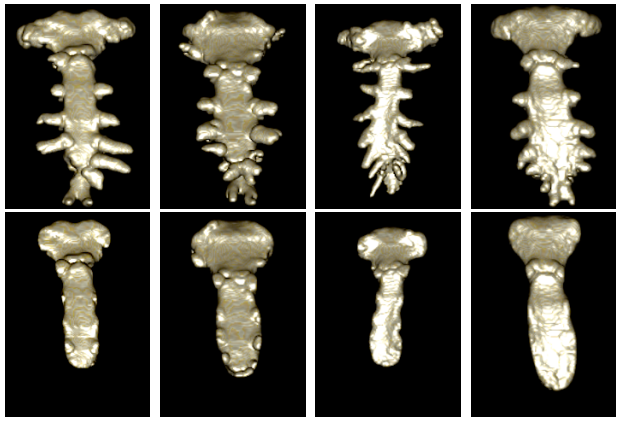

Fig. 4. Top row: Sternum segmentation in 4 patients' MDCT dataset with calcified costal cartilage. Bottom row: Results after removing calcified parts.

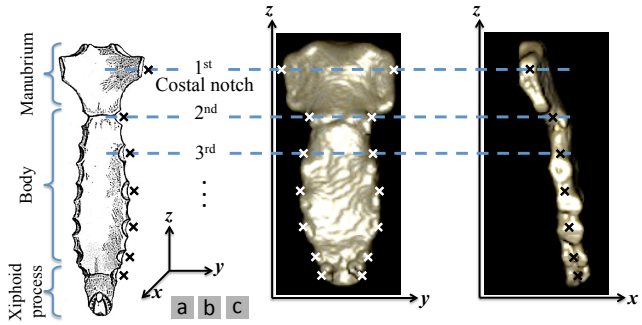

Fig. 5. (a) Sternum front-view [4] and manually marked costal notches, (b) and (c) 3-D costal notches positioning on sternum segmentation result

and determine 7 costal notches in the z direction (Figure 5.a).

The ratio of mask height to marked costal notches is used to determine the costal notches location in z direction on final sternum segmentation front-view (Figure 5.b).

The costal notches are determined in y direction as the leftmost and rightmost pixels of the sternum front-view (Figure 5.b). The costal notches in x direction are localized as the middle pixel of side-view, found at determined z directions (Figure 5.c).

III. EXPERIMENTAL RESULTS AND EVALUATION

Material: The proposed method was tested on 16 patient datasets, each with 380 slices on average. All datasets were provided by the radiology department of *Prince of Wales Hospital, Sydney, Australia*. MDCT images were taken from patients of both sexes with an average age of 65.5 years and for different clinical reasons. All images were taken with Toshiba Aquilion PRIME CT scanner in axial direction with 1 mm slice thickness, and were saved in DICOM format with non-contrast protocol.

Parameters setting: To convert DICOM images to a conventional image format, we set window level (WL)=300 and window width (WW)=1500. We determine the DICOM values interval of $[WL - WW/2\ ,\ WL + WW/2]$ for conversion to an intensity image and save it in PNG format.

To refine the sternum segmentation and isolation result, active contours is run twice with different parameters. Weight

DSC (%)	Sensitivity (%)	Specificity (%)	FNR (%)	FPR (%)	d_{mean} (mm)	d_{rms} (mm)
91.76	**92.49**	**99.51**	**7.51**	**0.49**	**1.07**	**1.72**

Where:
n: number of neighbors & M: mask & A: result of automatic algorithm
DSC (Dice similarity coefficient) = $(2\times|M \cap A|)/(|M| + |A|)$
Sensitivity = $TP/(TP + FN)$ & Specificity = $TN/(TN + FP)$
TP: true positive & TN: true negative & FP: false positive & FN: false negative
FNR: false negative ratio & FPR: false positive ratio
FNR = $1 - Sensivity$ & FPR = $1 - specificity$
pM: number of pixels defining M contour &
pA: number of pixels defining A contour

$$d_{mean} = \left(\sum_{q=1}^{pM} d(q,M) + \sum_{q=1}^{pA} d(q,A)\right)/(pM + pA)$$

$$d_{rms} = \sqrt{\left(\sum_{q=1}^{pM} d(q,M)^2 + \sum_{q=1}^{pA} d(q,A)^2\right)/(pM + pA)}$$

$$d(q,M) = min_r\left\{\sqrt{(x_q^A - x_r^M)^2 + (y_q^A - y_r^M)^2}\right\} \;\&$$

$$d(q,A) = min_r\left\{\sqrt{(x_r^A - x_q^M)^2 + (y_r^A - y_q^M)^2}\right\}$$

Fig. 6. Performance evaluation, tested on 16 datasets

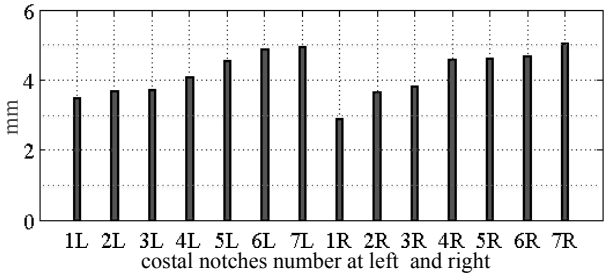

Fig. 7. 3-D Euclidean distance error of costal notches localization in 16 lung MDCT datasets, with 4.2 mm on average

of smoothing term and number of iterations for the first time running are set to 15 and 2000 respectively and for the second time are set to 30 and 1000.

Evaluation: The front-view of the sternum segmentation results were compared to the corresponding reference masks. The sternum reference masks were delineated by a trained radiologist on OsiriX output images. The xiphoid process was excluded from the reference mask, as the level of the xiphoid process calcification is variant in different individuals.

Performance of the proposed algorithm for sternum segmentation and comparisons of the results to the reference masks were evaluated using different criteria. A summary of the evaluations is shown in Figure 6.

To evaluate the costal notches localization, the positions of 14 costal notches for each dataset were manually marked in 3-D and confirmed by the trained radiologist. The 3-D Euclidean distance between the marked and automatically localized costal notches were measured individually. The average of the Euclidean distance error for 14 costal notches, calculated from 16 datasets, in shown in Figure 7.

IV. DISCUSSION

In this paper we present a novel fully automatic algorithm for 3-D segmentation of human sternum in MDCT images and 3-D positioning of costal notches. The evaluation shows high performance for segmentation and low distance error for costal notches positioning. To our knowledge, sternum segmentation has not been fully evaluated before.

The result of 3-D sternum segmentation can be useful in sternum implant surgeries as well as studies involving sternum geometry analysis [13]. It can assist cosmetic surgeons performing sternum deformities correction to visualize the sternum in 3-D and also in procedures predicting surgery outcome before the operation.

In most CT images, costal cartilages are low in contrast and the accurate costal notches positioning proposed here, will assist in prediction of costal cartilage centre points from CCJ to the sternum [3].

ACKNOWLEDGMENT

The authors would like to thank Dr. Daniel Moses of *Medical Imaging Department, Prince of Wales Hospital, NSW, Australia* for providing MDCT images for training and the reference markings that were used for testing and evaluation of this work.

REFERENCES

[1] M. Stojkovic, J. Milovanovic, N. Vitkovic, M. Trajanovic, N. Grujovic, V. Milivojevic, S. Milisavljevic, and S. Mrvic, "Reverse modeling and solid free-form fabrication of sternum implant," in *Australasian Physical and Engineering Sciences in Medicine*, vol. 33, 2010, pp. 243–250.

[2] S. Kido and A. Tsunomori, "Automated extraction of pleural effusion of three-dimensional thoracic ct images," in *Progress in Biomedical Optics and Imaging Proceedings of SPIE*, vol. 7260, 2009.

[3] A. Moreira, P. Rodrigues, J. Fonseca, A. Pinho, N. Rodrigues, J. Correia-Pinto, and J. Vilaa, "Pectus excavatum postsurgical outcome based on preoperative soft body dynamics simulation," in *Progress in Biomedical Optics and Imaging, Proceedings of SPIE*, vol. 8316, 2012.

[4] H. Gray and L. Warren Harmin, *Anatomy of the Human Body*, 20th ed. Philadelphia: Lea and Febiger: Bartleby, 2000.

[5] B. Pazokifard and A. Sowmya, "Efficient graph cuts based extraction of vertebral column and ribs in lung mdct images," international Conference on Image Processing, ICIP'13 (Submitted).

[6] A. Ali and A. Farag, "Automatic lung segmentation of volumetric low-dose ct scans using graph cuts," *Lecture Notes in Computer Science (in Artificial Intelligence and Bioinformatics)*, vol. 5358 LNCS, no. 1, pp. 258–267, 2008.

[7] Y. Boykov and M. P. Jolly, "Interactive graph cuts for optimal boundary and region segmentation of objects in n-d images," in *Proceeding ICCV'01*, 2001, pp. 105 –112.

[8] Y. Boykov and G. Funka-Lea, "Graph cuts and efficient n-d image segmentation," *International Journal of Computer Vision*, vol. 70, pp. 109–131, 2006.

[9] Y. Boykov and V. Kolmogorov, "An experimental comparison of min-cut/max- flow algorithms for energy minimization in vision," *Pattern Analysis and Machine Intelligence, IEEE Transactions on*, vol. 26, pp. 1124 –1137, 2004.

[10] M. Kass, A. Witkin, and D. Terzopoulos, "Snakes: Active contour models," *International Journal of Computer Vision*, vol. 1, pp. 321–331, 1988.

[11] V. Caselles, F. Catt, T. Coll, and F. Dibos, "A geometric model for active contours in image processing," *Numerische Mathematik*, vol. 66, pp. 1–31, 1993.

[12] V. Caselles, R. Kimmel, and G. Sapiro, "Geodesic active contours," in *Computer Vision, 1995. Proceedings., Fifth International Conference on*, jun 1995, pp. 694 –699.

[13] Z.-G. Chu, J.-Q. Yu, Z.-G. Yang, L.-Q. Peng, H.-L. Bai, and X.-M. Li, "Correlation between sternal depression and cardiac rotation in pectus excavatum: Evaluation with helical ct," *American Journal of Roentgenology*, vol. 195, no. 1, pp. W76–W80, 2010.